A Novel Deep Learning Approach for Colon and Lung Cancer Classification Using Histopathological Images

Naeem Ullah
Department of Electrical Engineering and Information Technology
University of Naples "Federico II"
Naples, Italy
naeemullahfeb1997@gmail.com

Ivanoe De Falco
Institute for High-Performance Computing and Networking (ICAR)
National Research Council (CNR)
Naples, Italy
ivanoe.defalco@icar.cnr.it

Giovanna Sannino
Institute for High-Performance Computing and Networking (ICAR)
National Research Council (CNR)
Naples, Italy
giovanna.sannino@icar.cnr.it

2023 IEEE 19th International Conference on e-Science (e-Science) | 979-8-3503-2223-1/23/$31.00 ©2023 IEEE | DOI: 10.1109/E-SCIENCE58273.2023.10254909

***Abstract*—Colon and Lung cancers are two of the most common causes of mortality in adults. They may simultaneously form in organs and have a detrimental effect on human life. There is a high risk that cancer will spread to the two organs if it is not discovered in the early stages. One of the most essential elements of successful therapy is the histological diagnosis of such cancers. Deep learning algorithms have improved the speed and accuracy of time-consuming and challenging procedures, enabling researchers to examine a huge number of patients swiftly and inexpensively. By examining their histological images and applying modern deep learning, this study develops a classification framework called DeepLCCNet to discriminate between five kinds of colon and lung tissues (three malignant and two benign). More precisely, we have classified five tissue types of Lung and Colon Cancer Histopathological Images data set using our model, i.e., benign tissue of the lung, squamous cell carcinoma of the lung, adenocarcinoma of the lung, benign tissue of the colon, and adenocarcinoma of the colon. According to the results, the proposed model can detect cancer tissues with an average accuracy of 99.67% and maximum accuracy of 99.84%. Medical professionals will be able to utilize a precise, automated system for detecting and classifying various kinds of colon and lung cancers.**

***Index Terms*—colon cancer, DeepLCCNet, deep learning, histopathological images, lung cancer**

I. Introduction

Cancer is one of the prevalent reasons for fatalities around the globe, according to the World Health Organization (WHO). Colon and lung cancers are among the major causes of death among afflicted organs. Across the globe, colon cancer causes 9.2% of all cancer-related fatalities, compared to lung cancer's 18.4% [1], [2] prevalence. About 17% of cases of lung and colon cancer develop together. Whereas this rate is unusual, in the absence of prompt discovery, cancer cells are highly probable to migrate across these two organs [3]. The major kind of colon cancer, colon adenocarcinoma, accounts for more than 95% of cancer cases. Adenocarcinoma is a specific kind of polyp (tissue growth) termed an adenoma that eventually transforms into cancer inside the large intestine. Lung adenocarcinomas make up around 40% of lung cancers and are more common in females than males. Some tumors are categorized as benign tumors and often pose no threat to life. Another kind of small cell cancer that grows in the bronchi or airways of the lung is lung squamous cell carcinoma. It makes up around 30% of all instances of lung cancer and is the second major and most common kind. The only approaches to minimize death from cancer at this time are early detection and quality care [4]. It is true that a person's chances of survival and recovery increase with the better treatment they receive and the earlier they are diagnosed.

Cancer development may be influenced by a high BMI, cigarette, alcohol, and other behavioral characteristics. Radiation, UV light, and a few biological and genetic ones are physical carcinogens [5]. Pain, nausea, exhaustion, shortness of breath, weight loss, persistent cough, hemorrhage, muscle aches, and bruises are all signs of cancer [6]. None of these symptoms, however, are exclusive to cancer and neither are they experienced by all patients. When people first develop signs of the disorder, they typically do so slowly or not at all, but by the time they do, it is frequently too late. Due to the high cost of these screening tools for standard tests, many people cannot afford them. According to the WHO, 70% of cancer-related fatalities are found in middle- and low-income nations [5]. These nations must construct a sizable number of diagnostic centers and laboratories with the educated medical staff and necessary tools to carry out diagnostic operations. Furthermore, people who are poor must be capable to pay for these evaluations.

In order to detect cancer cells and check out any other potential illnesses, doctors do sputum cytology, tissue collection (biopsy), imaging techniques (X-Ray, CT scan), and other operations. During the biopsy, competent pathologists must examine the microscopic histopathology slides to make the diagnosis [6] and identify the many kinds and sub-kinds of malignancies [7]. To identify colon and lung cancers, this work exclusively uses histology scans. Histopathological images are vital for determining a patient's prognosis and are frequently utilized by medical practitioners for examination. By examining histological images, health professionals have

traditionally undergone a time-consuming process to detect cancer; however, with the use of modern technology tools, this approach may now be accomplished with less effort and time. Systems that use artificial intelligence (AI) are widely recognized for their capacity to swiftly analyze data and draw conclusions. Recently, a number of CAD tools have been created to automatically check the colon and lungs for tumor or malignant growth [8]. Machine learning (ML) and deep learning (DL) techniques from the examination of histopathological images are the two most widely used AI approaches for discovering colon and lung cancer. Diagnostic systems may now properly identify cancer thanks to AI.

Recent research in this area has demonstrated successful colon and lung cancer detection using ML. However, pre-processing (to eliminate noise), feature extraction (to extract distinctive characteristics), feature selection (to pick essential features), optimization, and ultimately classification were the phases employed in ML techniques. When employing huge amounts of data, ML-based cancer diagnosis systems are more difficult and time-consuming since they require human feature recognition and distinct classifiers for the detection. When used with massive data, the majority of these algorithms also have overfitting issues and low accuracy levels. On the other hand, DL techniques substantially reduce the negative effects of earlier ML approaches. In these methods, the deep model is used to merge the feature extraction and classification steps into one stage. Pre-trained models and transfer learning (TL) techniques were frequently used by the researchers that used systems-based DL approaches; however negative transfer and overfitting are the two key downsides of these strategies. Many works of literature have used a variety of DL applications for medical image analysis, including brain tumor identification, COVID detection, and many forms of cancer detection. Big data is frequently required by these DL-based cancer detection algorithms. Due to the deep approaches' capacity to extract potent high-level features, they were capable of attaining greater accuracy on huge data than ML methods. In this research, we proposed a brand-new CNN-based DL method for the classification of colon and lung tumors. The work's key objectives are:

- For the classification of colon and lung cancers, we created and deployed a completely automated end-to-end Deep lung and colon cancer DL network (DeepLCCNet).
- A typical Kaggle data set named Lung and Colon Cancer Histopathological Images data set (LC25000) [9] with five classifications (benign tissue of the lung (LBT), squamous cell carcinoma of the lung (LSCC), adenocarcinoma of the lung (LAC), benign tissue of the colon (CBT), and adenocarcinoma of the colon (CAC)) is used in thorough tests to demonstrate the superiority of our system over existing methods for the classification of colon and lung cancer.
- We compared the classification performance of the DeepLCCNet framework with hybrid approaches on a similar data set and experimental setting.

The remaining article is structured as follows. The current literature in this field is provided in Section 2. Section 3 details the proposed approach. Section 4 provides the details of the data set used to evaluate our method, Section 5 provides an explanation of the findings, and a discussion of the comparison between our method and current state-of-the-art approaches. In Section 6, the planned study is concluded.

II. Related Work

The majority of recent research [8]– [10] concentrated on the use of ML, TL, and DL to categorize colon and lung cancer from the study of histopathological images.

The researchers in [8] utilized the 7180-photo IoT database CRC-VAL-HE-7K, which is openly accessible, to recognize colon cancer tissues on histopathology images. Feature extraction is possible by using Differential-Box-Count on each block of the image. ML methods utilized to analyze the data set include Extreme Gradient Boosting (EGB), K-Nearest Neighbor, Gaussian Naive Bayes, Random Forest (RF), Decision Tree, and Support Vector Machine (SVM). Results show that EGB is the most efficient and useful technique.

By looking at their histopathological images, the authors of [11] used an ML approach that can effectively categorize the images of the LC25000 data set into five different kinds of lung and colon tissues (two categories for colon and three categories for lung cancer). The different frameworks including SVM, XGBoost, RF, and other image processing methods are used to classify histopathological images of colon and lung tumors that were derived from the LC25000 data set. The obtained experimental outcomes showed that ML frameworks are very effective in categorizing colon and lung cancer subtypes and offer good results. The XGBoost framework performed the best when compared to other models.

In [12], the authors created a new supervised learning strategy based on DL that recognizes five various tissue types that exist in colon and lung tumors (three carcinogenic, two non-cancerous). They utilized the LC25000 database to evaluate their approach. For the classification of images, four sets of characteristics were produced employing two different domain transformations. To develop a combined collection of features that includes both kinds of information, the collected features were combined.

Six feature extraction methods based on color, shape, structure, and texture were utilized by the authors of [13] to identify handcrafted elements. Handmade feature-based Gradient Boosting (GB), SVM Radial Basis Function (SVM-RBF), RF, and Multilayer Perceptron (MLP) classifiers are evaluated for the categorization of colon and lung cancer. In a separate method that makes use of the idea of transfer learning, seven DL models were utilized for deep feature extraction from images of colon and lung cancer histology. The standard GB, MLP, RF, and SVM-RBF classifiers are applied with the recovered deep features (as input characteristics) for the categorization of colon and cancer. However, compared to manually created features, classifier performance is observed

to dramatically improve when employing features derived by deep CNN networks.

Using histopathology images, an AI-supported framework, and optimization approaches, the authors of [3] demonstrated how to identify colon and lung cancer. An SVM was employed to classify the features extracted using the DarkNet-19 framework (trained from scratch).

A substantial set of images from colon and lung histology were employed in [14] for training and validation. They used an LC25000 data set which is uniformly distributed into five groups. Four of the layers of a pre-trained neural network (AlexNet) were altered before the network was trained on the data set in order to fine-tune it. The preliminary classification findings, with the exception of one class of photographs, were positive. In order to raise overall performance and retain the framework's computational efficiency, the image quality from the ineffective category was enhanced by employing a simple and effective contrast enhancement approach.

The authors of [15] suggested a computer-aided diagnostic approach to recognize colon and lung cancer tissues on the LC25000 database. They used three pre-trained DL frameworks: GoogLeNet, ResNet18, and ShuffleNet V2 as well as one simple customized CNN algorithm. ShuffleNet V2 needed the least amount of training time, whereas ResNet18 had the best classification accuracy for lung cancer.

The LC25000 data set was utilized by the authors of [16] and used all 25,000 images including healthy cells and colon and lung cancers. Lung cancer images were not examined in this work since the major focus was on colon cancer. The colon's adenocarcinomas and benign cells were identified on histology slides using CNN architecture.

In [10], a CNN model was proposed that can more accurately identify and categorize various kinds of lung cancer, which is essential for treatment. They used the LC25000 data set and examined adenocarcinoma, squamous cell carcinoma, and benign tissue, i.e., the three primary types of lung tissues. 50 histopathological images from each group were used in the testing phase. The outstanding data were separated into training and validation groups, which included around 80% and 20% of data, respectively.

A review of past studies has revealed substantial issues with the automated algorithms now in use for classifying colon and lung cancer. Some methods of identifying colon and lung cancer cannot be entirely automated because they require human-chosen criteria. DL approaches are becoming more and more popular since they can automatically extract features, but they also use a lot of memory and processing power. Additionally, colon and lung cancer detection technologies cannot perform well in terms of detection and classification. In order to solve the issues with colon and lung cancer categorization, we developed an effective and novel end-to-end DL framework. The categorization performance of the lung and colon is enhanced by our proposed DL-based approach.

III. Methodology

The application of deep learning methods has now substantially helped the areas of image processing and medical image analysis (more specifically, medical histopathology image classification). In this work, we present the DeepLCCNet DL method for histopathology image-based identification of lung and colon cancer. We will categorize images into five classes (three malignant and two benign) using the LC25000 data set. The abstract picture of the suggested strategy is shown in Figure 1.

A. Image Resizing

The histopathology images used as input measure 768×768 pixels. We performed some pre-processing to scale the histopathology images to 227×227 pixels in line with the requirements (input) of the DeepLCCNet framework in order to ensure consistency and speed.

B. 5-Fold Cross Validation

5-fold cross-validation (K-fold) is used to train our DeepLCCNet model. The data set will be split into five equal parts due to the usage of K-fold cross-validation, and the testing set will be different each time. The process will be repeated five times. The testing will gradually alter for the third, fourth, and fifth testing sets of data as well. For the first training of our model, the first fold, or the first 20% of the data, will serve as the testing set. The next four-folds, or the remaining 80% of the data, will be used to train our model. It is important to note that the data set will always consist of 80% training data and 20% testing data.

C. DeepLCCNet Architecture Details

In this research, the DeepLCCNet model for lung and colon histopathological image classification is proposed. Only 20 learned layers including 18 convolution (Conv) layers and 2 FC layers, make up the DeepLCCNet framework. Overall, there are 66 layers in our model: one input layer, 12 for convolution, 6 for group convolution, two for cross-channel normalization (CCN), 19 for leaky rectified linear unit (LReLU), four for maximum pooling, 17 for batch normalization (BN), two for fully connected (FC), one for dropout (DO), one for softmax, and one for classification. The LReLU activation function is applied after convolution and group Conv layers.

We used two Fire modules in our framework. The Fire module consists of three Conv layers: a squeeze Conv layer with several 1×1-kernel layers, followed by expand layers which consist of both 1×1 and 3×3 Conv layers. We selected a 1×1 layer to lower the number of parameters. The total number of parameters in the layer is determined by multiplying the number of input channels by the quantity of kernels and the dimensions of the filters (i.e., 3). In order to minimize the amount of inputs (input channels) to 3×3 filters, we employed fewer filters in the squeeze layer than in the expanding layer. Furthermore, to make the results of the 1×1 and 3×3 kernels the same dimensions, we employed 1-pixel padding in the Conv layers with 3×3 kernels.

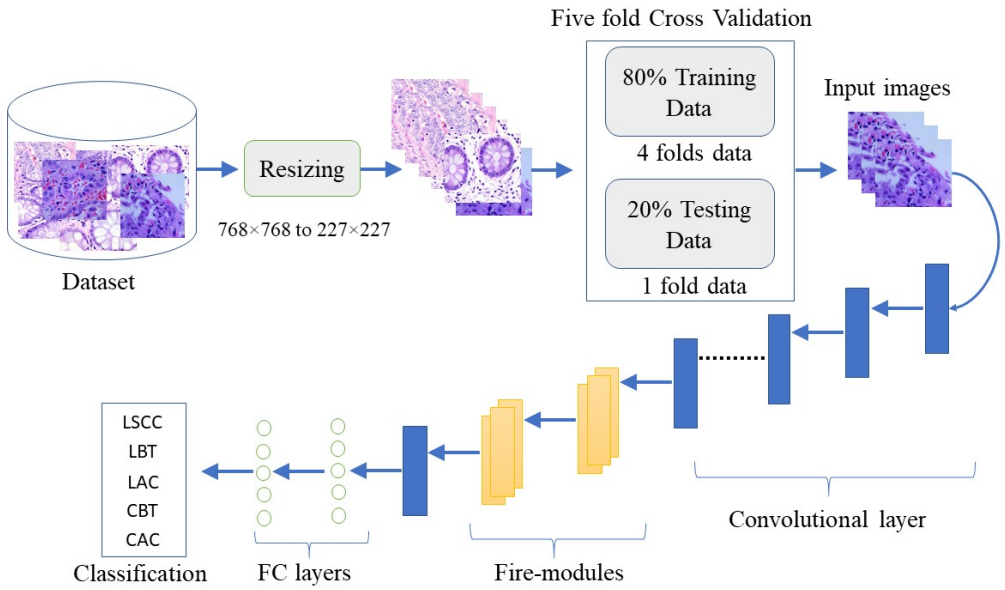

Fig. 1. Workflow of the proposed system.

Additionally, we used both CNN [17] and BN [18] operations in our framework. The included CNN layer drops both top-5 and top-1 error rates and improves generalization [17]. The BN layer was included because it speeds up model training by decreasing internal covariate shifting [19]. BN operation stabilizes CNN frameworks and maintains data distribution or data dispersion. As we train the DeepLCCNet DL model, the input distribution changes, which slows down model training (internal covariate). We use BN to cope with covariate shifting while maintaining the same data distribution (mean = 0, standard dev = 1). Even though some categorization characteristics have a larger numerical value than others, BN normalizes each feature while maintaining its relevance. The suggested network will be impartial (to larger-value categorization features) as a consequence. Furthermore, the model using this method is trained quicker and has greater accuracy compared to a network that does not use BN. BN is performed after each Conv layer to regularize the inputs, offer regularization, speed up neural network learning and aid in avoiding overfitting, and minimize the generalization error (enhance the generalization capability of the network).

The activation functions are placed after every Conv and group Conv layer. The activation functions come after convolutional layers. In the past, the tanh and sigmoid activation functions were the most common. The ReLU and its variants (LReLU, Noisy ReLU, and ELU), which are currently used in the majority of DL approaches, were created as a result of these restrictions. The weighted sum of the input is converted into output by a node in a layer using the ReLU. The ReLU activation function deactivates all neurons with negative values, making a sizable chunk of the network inactive. Instead of specifying that the ReLU activation function be 0 for negative input values, we utilized an improved version of ReLU (LReLU) to define the ReLU as a very tiny linear fraction of x. This improved activation function improved the model's classification performance [20]. The LReLU was determined as follows: In distinction to ReLU, the LReLU also produces an output for negative values and does not deactivate the inputs.

The DeepLCCNet framework's architecture is displayed in Table I. The input layer is the initial (top) layer in the DeepLCCNet model. Its dimensions are the same as the input features' dimensions, and it has I×J units. Our model supports input pictures with 227×227-pixel dimensions for processing. In order to construct the feature maps, Conv layers with kernel sizes of 11×11, 5×5, 3×3, and 1×1 are employed. The first Conv layer uses 96 kernels of size 11×11 with a shift of 4×4 to extract the feature from the input picture (of size 227×227). After applying convolutions and a kernel, the Conv layers' output (a feature map) is obtained as given in eq (1). The following formula denotes the convolution procedure between the filter and image:

$$\mathrm{f}_c^k(m,n) = \sum_d \sum J_d(r,s).\mathrm{i}_c^k(v,w) \tag{1}$$

f_c^k denotes the resulting feature map, $J_d(r,s)$ denotes the histopathological image which is multiplied by $i_c^k(v,w)$ index of the *kth* filter of the cth layer. After using convolutions on the histopathological images, the result of size *o=((i-k)+2p)/(s+1)* is created, where input is denoted by *i*, padding is represented by *p*, kernel size is denoted by *k*, and steps are represented by *s*. The Conv layers are followed by CNN or BN and LReLU activation functions. The LReLU activation functions work as follows:

$$f(x) = max(0.01 \times x, x) \tag{2}$$

The LReLU provides the result x when given a positive input, but 0.01 times x (a tiny number) when given a negative input.

We used the maximum pooling layer (Max-pool) after the first, second, fourteenth, and eighteenth Conv layers. The Max-pool with a shift of 2×2 is employed for downsampling. This layer reduces the amount of space, processing, parameters, and computations. The Max-pool layer works as follows

$$f(x) = \mathrm{x}_1, \mathrm{x}_2, \mathrm{x}_3, \mathrm{x}_4, ..., \mathrm{x}_k \tag{3}$$

The best possible feature map is represented by *f(x)*. In our model, the maximum value from the nearest pixels (in a histopathological image) is chosen to utilize Max-pool, employing a filter of size 3×3 and a shift of size 2×2.

After utilizing the activation function (LReLU) and CCN, the resulting feature of the first Conv layer is sent to the second Conv layer (i.e., group Conv layer) having 128 filters of size 5×5 and padding 2×2. The second layer is also followed by LReLU, CNN, and Max-pool. Similarly, the second Conv layer's resulting features are utilized as input to the third Conv layer, and so on. All the layers are connected sequentially.

The result of the final Conv layer—the eighteenth—is sent to the first FC layer. The 2-D feature map that was generated from the convolution layers is converted into a 1-D feature vector by the FC layer. The following are the functions of an FC layer.

$$\mathrm{a}_i = \sum_{j=0}^{m \times n-1} \mathrm{w}_{ij} \times \mathrm{x}_i + \mathrm{b}_i \tag{4}$$

where *b*, *i*, *n*, *m*, *w*, and *d* denote the bias, output index, height, width, weights, and depth of the FC layer, respectively. To prevent the issue of overfitting we utilized the DO after the first FC. The second FC layer is followed by 5-way softmax and classification layers. The output of the final FC layer is routed to a 5-way softmax due to the five categories in the LC25000 data set.

D. Hyper-parameters

The success of DL networks is dependent on the choice of the best hyper-parameters. To find the optimal values for all hyper-parameters considering multiple possibilities, we inspected the success of the recommended DeepLCCNet architecture employing different numbers of hyper-parameters. Table II displays the final values of the hyper-parameters. The stochastic gradient descent optimization technique (SGDM) was employed since it is rapid, memory-efficient, and better suited for larger data sets. To avoid the problem of overfitting, we evaluated the framework for 10 epochs.

IV. DATA SET

We assessed our model on the colon and Lung cancer histopathological images database [9] (also known as LC25000). There are five classes and 25,000 histopathology images in this collection. Each image has 768 × 768 dimensions and is stored as a JPEG file. The current version of the database has five categories, i.e., Lung adenocarcinoma (LAC), Colon adenocarcinoma (CAC), Lung benign tissue (LBT), Lung squamous cell carcinoma (LSCC), and Colon benign tissue (CBT) each with 5,000 images. Some examples of images contained in the considered database are reported in Figure 2. Original pictures for the LC25000 data set were gathered at the Tampa, Florida-based James A. Haley Veterans Hospital. The authors primarily collected 1250 images of cancer tissues using pathology glass slides (250 images of each class). They increased the database to 25,000 images (5000 photos in each class) by utilizing image augmentation procedures to rotate and flip the genuine images under different circumstances. Before employing the augmentation procedures, the images were cropped to a square of 768 × 768 dimensions from their actual size of 1024 × 768 pixels. Each image in the data set has been confirmed, is compliant with the Health Insurance Portability and Accountability Act (HIPAA), and is accessible for unrestricted use.

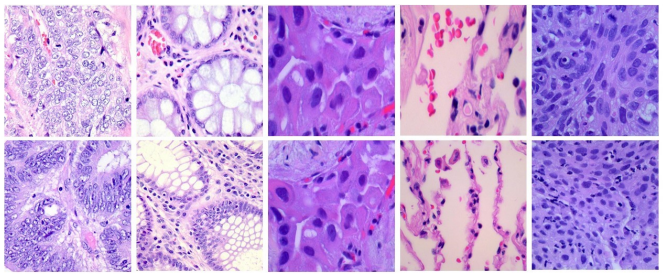

Fig. 2. Sample histopathological images of the data set, the first, second, third, fourth, and fifth columns has CAC, CBT, LAC, LBT, and LSCC respectively

V. RESULTS AND DISCUSSIONS

This part carefully examines the findings of the many tests that were run to see how well our model functions. We provide an overview of the performance measures and experimental techniques we utilized to gauge the effectiveness of our method.

A. Evaluation Metrics

With the use of the measures for sensitivity, precision, F1-score, and accuracy, we assessed the performance of our approach. The formulas for these metrics are as follows:

$$Accuracy = (TN + TP)/TS \tag{5}$$

$$Precision = TP/(TP + FP) \tag{6}$$

$$Sensitivity(recall) = TP/(TP + FN) \tag{7}$$

$$F1 - Score = 2 \times \frac{(Precision \times Recall)}{(Precision + Recall)} \tag{8}$$

where TN, TP, FP, FN, and TS stand for the true negative, true positive, false positive, false negative, and total number of samples, respectively.

TABLE I
DEEPLCCNET ARCHITECTURE DETAILS

S No	Operation	Layers	No of filters	Filter size	Stride	Padding
1		Input				
2	Conv	Conv (LReLU + CNN)	96	11×11	4×4	
3	Pooling	Maximum pooling		3×3	2×2	
4	Conv	GConv (LReLU + CNN)	128	5×5		2×2
5	Pooling	Maximum pooling		3×3	2×2	
6	Conv	Conv (LReLU + BN)	64	3×3		2×2
7	Conv	Conv (LReLU + BN)	64	3×3		2×2
8	Conv	Conv (LReLU + BN)	64	3×3		2×2
9	Conv	Conv (LReLU + BN)	64	3×3		2×2
10	Conv	GConv (LReLU + BN)	68	1×1		
11	Conv	GConv (LReLU + BN)	272	3×3		1×1
12	Conv	GConv (LReLU + BN)	68	1×1		
13	Conv	Conv (LReLU + BN)	384	3×3		1×1
14	Conv	Conv (LReLU + BN)	192	3×3		1×1
15	Fire module	Conv (LReLU + BN)	32	1×1		
16	Fire module	Conv (LReLU + BN)	128	3×3		1×1
17	Fire module	Conv (LReLU + BN)	128	1×1		
18	Pooling	Maximum pooling		3×3	2×2	
19	Fire module	Conv (LReLU + BN)	48	1×1		
20	Fire module	Conv (LReLU + BN)	192	1×1		
21	Fire module	Conv (LReLU + BN)	192	3×3		1×1
22	Conv	GConv (LReLU + BN)	128	3×3		1×1
23	Pooling	Maximum pooling		3×3	2×2	
24	FC + LReLU + BN + DO					
25	FC + Softmax + Classification					

TABLE II
HYPER PARAMETERS OF THE PROPOSED ARCHITECTURE

Parameters	Values
Learning rate	0.001
Shuffle	Every epoch
Optimization algorithm	SGDM
Maximum Epochs	10
AF	LReLU
DO	0.5
K-fold	5
Iterations per epoch	42
Verbose	true
Validation frequency	30

TABLE III
DETAILS OF THE SYSTEM USED FOR IMPLEMENTATION

Name	Experiment Parameters
ROM	500GB
CPU	Intel (R) Core (TM) i5-5200U
Development tool	MATLAB R2020a
RAM	8GB
Type of System	64-bit, Windows 10

B. Experimental Setup and Evaluation

On a laptop with an Intel (R) Core (TM) i5-5200U CPU and RAM of 8GB, we conducted all of the studies. MATLAB R2020a was used to carry out the strategy (Table III). For each experiment, the database is separated into testing and training sets. To find how well our suggested framework classifies histopathological images, we run a number of tests.

C. Performance Evaluation

This experiment's main objective is to demonstrate the usefulness and value of our method for locating and categorizing colon and lung malignancies. In this study, we used 5000 histological pictures of each class (LBT, LSCC, LAC, CBT, and CAC) from the Lung and Colon Cancer histological pictures collection, totaling 25,000 histopathological images of five classes. We employed five-fold cross-validation, in which the 25,000 photos were used for training across the five rounds. More specifically, in each round, we used 20,000 histopathology images of the colon and lungs to train our model, whereas 5000 images are used to validate our model. We trained our DeepLCCNet model utilizing the training set on the experimental settings provided in Table II for categorizing five classes of colon and lung cancer histopathology pictures. For colon and lung cancer categorization, our DeepLCCNet model required 3334 minutes and 45 seconds of training time. With optimal average accuracy, precision, recall, and F1-score values of 99.67%, 99.12%, 99.04%, and 99.08%, the proposed framework correctly divided colon and lung diseases into several groups. The proposed framework achieved maximum

accuracy, precision, recall, and F1-score values of 99.84%, 99.4%, 99.4%, and 99.4% in fold 2. According to the results (Table IV), the DeepLCCNet model can correctly classify most of the colon and lung cancer histopathological images. Our method produces the best results with a high TP rate for all of the cancer classes in our data set since the proposed framework accurately identified the majority of the cancer categories' image samples.

TABLE IV
FIVE-FOLD CROSS-VALIDATION RESULTS ACHIEVED BY OUR DEEPLCCNET

Number of the fold	Accuracy	Precision	Recall	F1-score
1	99.57	99.00	99.00	99.00
2	99.84	99.40	99.40	99.40
3	99.68	99.20	99.00	99.10
4	99.92	99.40	99.40	99.40
5	99.36	98.60	98.40	98.50
Average	99.67	99.12	99.04	99.08

To estimate the usefulness and reliability of the proposed strategy, accurate colon and lung cancer diagnosis, detection, or classification is required. To do this, we assess the class-wise performance of the DeepLCCNet technique in identifying various cancer types. The effectiveness of the proposed DeepLCCNet technique for identifying each cancer type is revealed in Tables V to IX in terms of F1 score, precision, accuracy, and recall. The suggested approach gives a state-of-the-art performance in each assessment criterion, according to the results. The findings show that most images are accurately detected, enhancing accuracy. The new framework's robustness, which more properly represents each class, is the key component in the greater accuracy of identifying colon and lung cancers.

TABLE V
CLASS-WISE PERFORMANCE OF THE PROPOSED DEEPLCCNET ARCHITECTURE IN FOLD 1

Class	Accuracy	Recall	Precision	F1-score
CAC	99.77	99.00	100.00	99.50
CBT	99.77	100.00	99.00	99.50
LAC	99.17	97.00	99.00	98.00
LBT	99.96	100.00	100.00	100.00
LSCC	99.21	99.00	97.00	98.00

TABLE VI
CLASS-WISE PERFORMANCE OF THE PROPOSED DEEPLCCNET ARCHITECTURE IN FOLD 2

Class	Accuracy	Recall	Precision	F1-score
CAC	99.98	100.00	100.00	100.00
CBT	100.00	100.00	100.00	100.00
LAC	99.93	98.00	99.00	98.50
LBT	100.00	100.00	100.00	100.00
LSCC	99.32	99.00	98.00	98.50

TABLE VII
CLASS-WISE PERFORMANCE OF THE PROPOSED DEEPLCCNET ARCHITECTURE IN FOLD 3

Class	Accuracy	Recall	Precision	F1-score
CAC	99.69	100.00	98.00	99.00
CBT	99.69	99.00	100.00	99.50
LAC	99.50	99.00	98.00	98.50
LBT	99.98	100.00	100.00	100.00
LSCC	99.52	98.00	99.00	98.50

TABLE VIII
CLASS-WISE PERFORMANCE OF THE PROPOSED DEEPLCCNET ARCHITECTURE IN FOLD 4

Class	Accuracy	Recall	Precision	F1-score
CAC	99.92	100.00	100.00	100.00
CBT	99.92	100.00	100.00	100.00
LAC	99.38	99.00	99.00	99.00
LBT	100.00	100.00	100.00	100.00
LSCC	99.38	98.00	98.00	98.00

Receiver Operating Characteristic (ROC) curve, shown in Figure 3, illustrates how well the DeepLCCNet architecture classifies colon and lung tumors. We made use of the MATLAB function per curve to calculate the ROC. The ROC produces results in the [0, 1] range using threshold values. For all threshold values, the TP Ratio and FP Ratio are considered. The ROC curve displays the FP to TP ratio, representing the algorithm's sensitivity. One of the most important evaluation criteria for algorithms is the area under the curve (AUC), which quantifies how different classes differ from one another. It controls how well the algorithm can differentiate between classes. If the AUC value is near to 1, the framework will be more successful in distinguishing between different illness types. The AUC rating of our model was 0.9999.

We conducted an analysis to identify the reason of DeepLCCNet model achieved the best results and found the following reasons. We used small filters of size 1×1 and 3×3 to extract more detailed features. In order to both high-level and low-level feature maps, Conv layers with kernel sizes of 11×11, 5×5, 3×3, and 1×1 are employed. To increase the training speed of our model, normalize features, make the network more stable, minimize the training epochs, and reduce overfitting by offering some regularization, batch normalization is

TABLE IX
CLASS-WISE PERFORMANCE OF THE PROPOSED DEEPLCCNET ARCHITECTURE IN FOLD 5

Class	Accuracy	Recall	Precision	F1-score
CAC	99.32	99.00	97.00	98.00
CBT	99.32	98.00	99.00	98.50
LAC	99.09	100.00	96.00	98.00
LBT	100.00	100.00	100.00	100.00
LSCC	99.09	96.00	100.00	98.00

used. The LReLU Layer is used to expedite training while addressing the ”dying RelU” problem (no zero slopes in the case of LR). In order to lessen overfitting and co-adaptation, we employed a 50% dropout rate. Co-adaptation, which results in overfitting, occurs when multiple neurons in a layer extract deeply similar or identical characteristics from the input data.

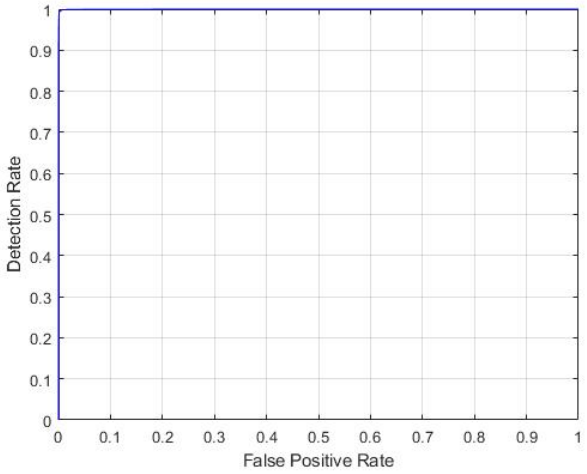

Fig. 3. ROC plot of the DeepLCCNet model.

D. Comparison With State-of-the-Art Deep Learning Models

This experiment's main goal is to demonstrate that the DeepLCCNet approach, which has been suggested, is more accurate than the currently available pre-trained DL models which can also be used for the categorization of colon and lung cancer. We used four pre-trained DL models, more specifically, Squeezenet [21], Efficientnetb0 [22], Resnet18 [23], Densenet201 [24], and Mobilenetv2 [25] to evaluate the proposed DeepLCCNet framework's classification performance. In a TL arrangement, the frameworks are trained on a large number of pictures from the ImageNet data set. Images may be categorized into 1000 different categories using pre-trained versions of all networks. The colon and lung cancer pictures are divided into five classes using the last three layers' fine-tuning. The models' picture input sizes varied, thus we scaled the data set's histopathology images in accordance with their requirements. To adjust the models, we used the same experimental setup as for the DeepLCCNet model that was suggested, as shown in Table II. For this experiment, we used the entire LC25000 data set of 25000 images. The proposed framework correctly classified colon and lung diseases into various groups, outperforming the other deep learning (DL) frameworks (as shown in Table X) by achieving the best average accuracy, precision, recall, and F1-score values of 99.67%, 99.12%, 99.04%, and 99.08%, respectively.

Since the ReLU activation function follows each convolutional layer in the other DL models used for comparison purposes, their accuracy is lower than that of the suggested model. All the neurons that have values lower than (x¡0), or negative values are always inactive. In this case, the optimization procedure fails, which prevents the model from learning. Because it causes a sizable portion of the network to gradually go dormant, the dying ReLU issue is troublesome. The dying relu problem is addressed by the proposed DeepLCCNet model by replacing ReLU with the Leaky ReLU activation function. The DeepLCCNet model maintains all neurons active and learns in the presence of negative values which results in improved performance. Additionally, we included CNN and BN layers in the suggested design. The top-1 and top-5 error rates are decreased and generalization is improved using the CNN layer [26]. By minimizing internal covariate shifting, BN expedites model training [27]. While retaining data dispersion (data distribution), BN can sustain DL models. As we train the DeepLCCNet DL model, the input distribution changes, which slows down model training (internal covariate). We use BN to cope with covariate shifting while maintaining the same data distribution (standard dev = 1, mean = 0). Even if some categorization features have a higher numerical value than others, BN normalizes each characteristic such that its relevance is preserved. The suggested network will be impartial (to higher-value categorization features) as a consequence. Additionally, a framework that makes use of this method trains more quickly and more accurately than one that does not.

TABLE X
COLON AND LUNG CANCERS CLASSIFICATION USING HISTOPATHOLOGICAL IMAGES COMPARISON WITH DL MODELS

Model	Accuracy	Precision	Recall	F1-score
Densenet20	92.42	91.00	92.00	91.50
Squeezenet	96.84	96.80	96.20	96.50
Efficientnetb0	97.50	97.08	96.80	96.93
Resnet18	98.90	97.60	97.80	97.70
Mobilenetv2	98.99	98.40	98.20	98.30
Proposed model	***99.67***	***99.12***	***99.04***	***99.08***

E. Comparison with State-of-the-art Approaches

To validate the strength of the proposed framework, we compared the proposed DeepLCCNet technique to the most contemporary methodologies, and the outcomes are shown in Table XI. In [28], the authors described the implementation of a unique model for the automated categorization of histological pictures pertaining to lung tissues. The color normalization approach was initially used to increase contrast in the histopathological pictures obtained from the LC25000 lung histopathology image collection. Furthermore, the feature vectors were extracted from the segmented histopathological pictures using the feature descriptors Alexnet and Grey Level Co-Occurrence Matrix (GLCM) features. Finally, for the best feature selection and lung tissue classification, the extended grasshopper optimization algorithm (EGOA) and RF model were applied. According to the simulation results, the EGOA-RF framework has an accuracy rate of 98.50% when applied to the LC25000 lung histopathology imaging data set. In

TABLE XI
COMPARISON WITH STATE-OF-THE-ART METHODS WHICH USE LC2500 DATA SET

Reference	Method	Accuracy	Date
Kumar et al. [13]	DenseNet-121 for feature extraction and RF for classification	98.60%	2022
Mehmood et al. [14]	Pre-trained Alexnet	89.00%	2022
Karim et al. [10]	CNN	98.07%	2021
Pradhan et al. [28]	Alexnet and GLCM for feature extraction and random forest for classification	98.50%	2023
Rajput et al. [29]	Pre-trained Resnet	98.57%	2023
Proposed method	***DeepLCCNet model***	***99.23%***	***2023***

[29], the authors applied several DL models and methods on histopathology images to identify lung cancer. These models attain extremely high accuracy and produce results in very less time. On the test data, an accuracy of 98.57% using a pre-trained ResNet model and a support vector machine is attained. The identical data set, 25000 histopathological pictures of colon and lung tissues evenly split into 5 sets, was utilized by the authors in [14]. In order to fine-tune a pre-trained neural network (AlexNet), four of its layers were changed before the network was trained on the data set. With an overall accuracy of 89%, the initial classification findings looked good for all picture classes except for one. Instead of applying image improvement methods to the entire data set to increase accuracy, the underperforming class's photos' quality was enhanced by using a contrast enhancement approach, which is both straightforward and effective. Implementing the suggested methods enhances overall accuracy from 89% to 98.4% and showed computational efficiency. In [10], the authors presented a CNN model to more precisely identify and classify different forms of lung cancer. A CNN model was proposed with 15,000 pictures divided into three categories—training, validation, and testing. The model's validation accuracy was 98.07% for three different types of lung tissues (squamous cell cancer, benign tissue, and adenocarcinoma).

VI. CONCLUSIONS

One of the top reasons for mortality globally is cancer, particularly lung and colon cancer. The survival rates can be greatly enhanced by a timely and precise examination of these cancers. Detecting colon and lung cancer correctly and effectively was the aim of this research. On an LC25000 data set of 25,000 histopathology images of colon and lung tissues, a unique DeepLCCNet DL model is created for this identification. The average and maximum accuracy of our suggested model were respectively 99.67% and 99.84%. For the detection of lung and colon cancer, the suggested approach is more reliable and effective than other prior DL models. For the accurate detection of lung and colon cancer, the proposed methodology performed better than cutting-edge techniques. We think that our proposed technique can be used to correctly diagnose various illnesses. When the pathologist examining the lung and colon cancer photographs requires insurance, our application may be helpful since it will aid in making the proper diagnosis. Although the numerical results are excellent, this approach does not give information to the doctors on the reasons why an image is considered a specific type of cancer (LBT, LSCC, LAC, CBT, or CDC), so it is of little help to them. To overcome this problem, the system must be transformed into an explainable one by adding posterior ways such as Grad-CAM and LIME to extract information on those reasons. This is an important step towards explainable AI, and we will deal with it in our future activity. We'll test our DeepLCCNet on various data sets in the future to see how it does at predicting illnesses. For the purpose of choosing the best features from the retrieved deep features, we will use our DL model in conjunction with one of the optimization approaches, such as a genetic algorithm. Furthermore, the dataset's picture count was increased by using data augmentation techniques. Data augmentation can be helpful for DL research, but the additional images that are created are fake and are alterations of the original image. The artificial intelligence system's reliability is badly impacted by the lack of original photos and the prevalence of augmented images. To provide findings that are more accurate, we will employ a lot of raw data that will be generated by integrating several databases.

ACKNOWLEDGMENT

REFERENCES

[1] A. Bermúdez, I. Arranz-Salas, S. Mercado, J. A. López-Villodres, V. González, F. Ríus, M. V. Ortega, C. Alba, I. Hierro, and D. Bermúdez, "Her2-positive and microsatellite instability status in gastric cancer—clinicopathological implications," *Diagnostics*, vol. 11, no. 6, p. 944, 2021.

[2] F. Bray, J. Ferlay, I. Soerjomataram, R. L. Siegel, L. A. Torre, and A. Jemal, "Global cancer statistics 2018: Globocan estimates of incidence and mortality worldwide for 36 cancers in 185 countries," *CA: a cancer journal for clinicians*, vol. 68, no. 6, pp. 394–424, 2018.

[3] M. Toğaçar, "Disease type detection in lung and colon cancer images using the complement approach of inefficient sets," *Computers in Biology and Medicine*, vol. 137, p. 104827, 2021.

[4] L. F. Sanchez-Peralta, L. Bote-Curiel, A. Picon, F. M. Sanchez-Margallo, and J. B. Pagador, "Deep learning to find colorectal polyps in colonoscopy: A systematic literature review," *Artificial intelligence in medicine*, vol. 108, p. 101923, 2020.

[5] N. Alimu, A. Maimaiti, M. Maimaitituerxun, H. Muertizha, A. Qukuerhan, Y. Yasheng, J. Yong, N. Mierzhamu, M. Mierzhakemu, A. Aierken, *et al.*, "Xrcc1 gene rs72484243 polymorphism is associated with increased laryngeal cancer risk," *Biochemical Genetics*, 2023.

[6] S. Prabhu, "Pathology of organ systems of the body," in *Textbook of General Pathology for Dental Students*, pp. 133–146, Springer, 2023.

[7] W. D. Travis, E. Brambilla, M. Noguchi, A. G. Nicholson, K. R. Geisinger, Y. Yatabe, D. G. Beer, C. A. Powell, G. J. Riely, P. E. Van Schil, *et al.*, "International association for the study of lung cancer/american thoracic society/european respiratory society international multidisciplinary classification of lung adenocarcinoma," *Journal of thoracic oncology*, vol. 6, no. 2, pp. 244–285, 2011.

[8] A. Tripathi, K. Kumar, A. Misra, and B. K. Chaurasia, "Colon cancer tissue classification using ml," *2023 6th International Conference on Information Systems and Computer Networks (ISCON)*, pp. 1–6, 2023.

[9] A. A. Borkowski, M. M. Bui, L. B. Thomas, C. P. Wilson, L. A. DeLand, and S. M. Mastorides, "Lung and colon cancer histopathological image dataset (lc25000)," *arXiv preprint arXiv:1912.12142*, 2019.

[10] D. Z. Karim and T. A. Bushra, "Detecting lung cancer from histopathological images using convolution neural network," in *TENCON 2021-2021 IEEE Region 10 Conference (TENCON)*, pp. 626–631, IEEE, 2021.

[11] A. Hage Chehade, N. Abdallah, J.-M. Marion, M. Oueidat, and P. Chauvet, "Lung and colon cancer classification using medical imaging: A feature engineering approach," *Physical and Engineering Sciences in Medicine*, vol. 45, no. 3, pp. 729–746, 2022.

[12] M. Masud, N. Sikder, A.-A. Nahid, A. K. Bairagi, and M. A. AlZain, "A machine learning approach to diagnosing lung and colon cancer using a deep learning-based classification framework," *Sensors*, vol. 21, no. 3, p. 748, 2021.

[13] N. Kumar, M. Sharma, V. P. Singh, C. Madan, and S. Mehandia, "An empirical study of handcrafted and dense feature extraction techniques for lung and colon cancer classification from histopathological images," *Biomedical Signal Processing and Control*, vol. 75, p. 103596, 2022.

[14] S. Mehmood, T. M. Ghazal, M. A. Khan, M. Zubair, M. T. Naseem, T. Faiz, and M. Ahmad, "Malignancy detection in lung and colon histopathology images using transfer learning with class selective image processing," *IEEE Access*, vol. 10, pp. 25657–25668, 2022.

[15] R. R. Wahid, C. Nisa, R. P. Amaliyah, and E. Y. Puspaningrum, "Lung and colon cancer detection with convolutional neural networks on histopathological images," in *AIP Conference Proceedings*, vol. 2654, AIP Publishing, 2023.

[16] M. Hossain, S. S. Haque, H. Ahmed, H. A. Mahdi, and A. Aich, *Early stage detection and classification of colon cancer using deep learning and explainable AI on histopathological images*. PhD thesis, Brac University, 2022.

[17] A. Krizhevsky, I. Sutskever, and G. E. Hinton, "Imagenet classification with deep convolutional neural networks," *Advances in neural information processing systems*, vol. 25, 2012.

[18] N. Ullah, J. A. Khan, L. A. Alharbi, A. Raza, W. Khan, and I. Ahmad, "An efficient approach for crops pests recognition and classification based on novel deeppestnet deep learning model," *IEEE Access*, vol. 10, pp. 73019–73032, 2022.

[19] S. Ioffe and C. Szegedy, "Batch normalization: Accelerating deep network training by reducing internal covariate shift," in *International conference on machine learning*, pp. 448–456, pmlr, 2015.

[20] N. Ullah, M. S. Khan, J. A. Khan, A. Choi, and M. S. Anwar, "A robust end-to-end deep learning-based approach for effective and reliable btd using mr images," *Sensors*, vol. 22, no. 19, p. 7575, 2022.

[21] F. N. Iandola, S. Han, M. W. Moskewicz, K. Ashraf, W. J. Dally, and K. Keutzer, "Squeezenet: Alexnet-level accuracy with 50x fewer parameters and¡ 0.5 mb model size," *arXiv preprint arXiv:1602.07360*, 2016.

[22] M. Tan and Q. Le, "Efficientnet: Rethinking model scaling for convolutional neural networks," in *International conference on machine learning*, pp. 6105–6114, PMLR, 2019.

[23] K. He, X. Zhang, S. Ren, and J. Sun, "Deep residual learning for image recognition," *CoRR*, vol. abs/1512.03385, 2015.

[24] G. Huang, Z. Liu, and K. Q. Weinberger, "Densely connected convolutional networks," *CoRR*, vol. abs/1608.06993, 2016.

[25] M. Sandler, A. Howard, M. Zhu, A. Zhmoginov, and L.-C. Chen, "Mobilenetv2: Inverted residuals and linear bottlenecks," in *Proceedings of the IEEE conference on computer vision and pattern recognition*, pp. 4510–4520, 2018.

[26] N. Ullah, J. A. Khan, S. Almakdi, M. S. Khan, M. Alshehri, D. Alboaneen, and A. Raza, "A novel coviddetnet deep learning model for effective covid-19 infection detection using chest radiograph images," *Applied Sciences*, vol. 12, no. 12, p. 6269, 2022.

[27] N. Ullah, M. Marzougui, I. Ahmad, and S. A. Chelloug, "Deeplungnet: An effective dl-based approach for lung disease classification using cris," *Electronics*, vol. 12, no. 8, p. 1860, 2023.

[28] M. Pradhan and R. K. Sahu, "Automatic detection of lung cancer using the potential of artificial intelligence (ai)," in *Machine Learning and AI Techniques in Interactive Medical Image Analysis*, pp. 106–123, IGI Global, 2023.

[29] A. Rajput and A. Subasi, "Lung cancer detection from histopathological lung tissue images using deep learning," in *Applications of Artificial Intelligence in Medical Imaging*, pp. 51–74, Elsevier, 2023.